



RESEARCH ACTIVITIES

Life and Coordination-Complex Molecular Science

Department of Life and Coordination-Complex Molecular Science is composed of four divisions of Biomolecular science, two divisions of Coordination molecular science and two adjunct divisions. Biomolecular science divisions cover the studies on the elucidation of functions and mechanisms for various types of sensor proteins, protein folding, molecular chaperone, and metal proteins. Coordination complex divisions aim to develop molecular catalysts for the transformation of organic molecules, activation small inorganic molecules, and reversible conversion between chemical and electrical energies. Interdisciplinary alliances in the Department aim to create new basic concepts for the molecular and energy conversion through the fundamental science conducted at each division.

Bioinorganic Chemistry of Novel Hemeproteins

Department of Life and Coordination-Complex Molecular Science
Division of Biomolecular Functions



AONO, Shigetoshi
YOSHIOKA, Shiro
ISHIKAWA, Haruto
SAWAI, Hitomi
TANIZAWA, Misako

Professor
Assistant Professor
IMS Research Assistant Professor
JSPS Post-Doctoral Fellow
Secretary

Hemeproteins are a typical metalloprotein, which show a variety of functions including oxygen storage/transport, electron transfer, redox catalysis with various substrates. Besides these traditional functions of hemeproteins, several new functions of hemeproteins have been found recently. Heme-based sensor proteins show a novel function of the heme prosthetic group, in which the heme acts as the active site for sensing the external signal such as diatomic gas molecules and redox change. Aldoxime dehydratase is another novel hemeprotein, in which the heme prosthetic group tethers the substrate for its dehydration reaction. Our research interests are focused on the elucidation of the structure-function relationships of these novel hemeproteins.

1. Structure and Function of Aldoxime Dehydratase Containing a Heme as the Active Site for Dehydration Reaction

Aldoxime dehydratase (Oxd) is a new heme-containing enzyme that works as a hydro-lyase. The enzymatic activity of Oxd is dependent on the oxidation state of the heme iron, though the reaction catalyzed by Oxd is not a redox reaction. Ferrous Oxd containing a Fe^{2+} -heme shows the enzymatic activity, but ferric Oxd containing a Fe^{3+} -heme does not. Previous spectroscopic analyses reveal a novel mechanism, where the change in the coordination mode of the substrate plays a crucial role for the regulation of the enzymatic activity. While the oxygen atom of aldoxime is coordinated to the ferric heme, the nitrogen atom of aldoxime is coordinated to the ferrous heme. The dehydration reaction proceeds only via N-coordinated substrate in the ferrous heme. The organic sub-

strate is directly coordinated to the heme iron in dehydration of aldoxime, which is a unique example among heme enzymes though the coordination of O_2 or H_2O_2 to the heme is well known in the heme-containing oxygenases, catalases, and peroxidases. It is proposed that the dehydration reaction of the heme-bound aldoxime proceeds in a general acid-base catalysis with a histidine working as a catalytic residue in the distal heme pocket. However, the detail reaction mechanisms remained to be elucidated mainly because the structural information of Oxd was lacking.

We have determined the crystal structures of Oxd from *Rhodococcus* sp. N-771 (OxdRE) in the substrate-free and substrate-bound forms. OxdRE formed a homodimer with non-crystallographic two-fold symmetry, consistent with previous gel filtration analyses results. Each monomer contained one heme molecule. The $\alpha 10$ helix of one monomer interacted with the $\alpha 10$ helix of the other to create the dimer interface, which was stabilized by hydrogen bonds and electrostatic interactions.

We could determine the crystal structure of the Michaelis complex of OxdRE by means of the unique property of OxdRE for the substrate binding. As the reaction spontaneously proceeds when mixing ferrous Oxd and the substrate, the crystallization of the substrate-bound OxdRE in the ferrous form (the Michaelis complex of OxdRE) is not possible by usual methods. However, we could prepare the crystal of the Michaelis complex of OxdRE by the reduction of the crystal of the substrate-ferric Oxd complex using X-ray irradiation under cryogenic temperature. The structures of the resting state and the Michaelis complex provide the structural insights into the mechanisms of substrate recognition and the catalysis of OxdRE.

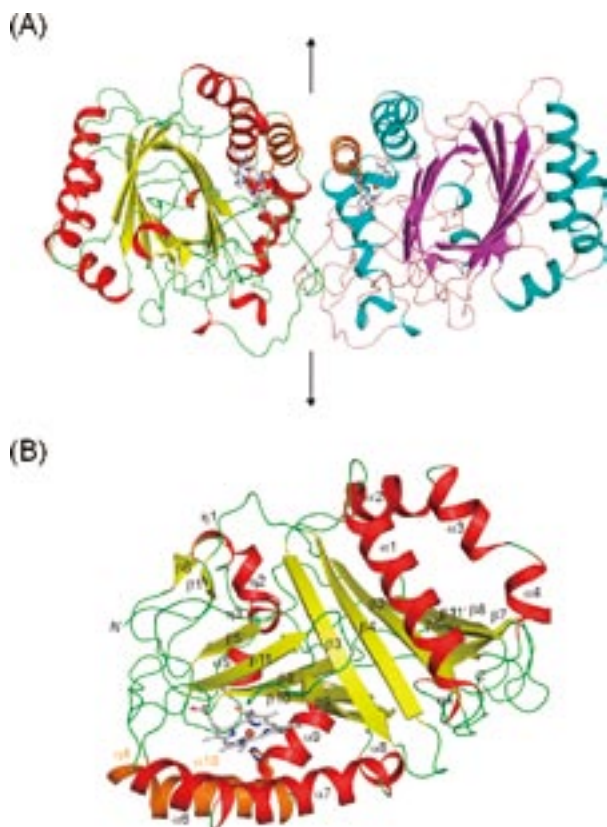


Figure 1. Crystal Structure of OxdRE in substrate-free form. The structures are colored based on the secondary structural elements. The heme is represented by a silver-colored stick model. The heme proximal helix (α 10), the subsequent 3_{10} helix (η 4), and the axial His299 are colored in orange. (A) Structure of the OxdRE dimer. Two subunits are related by non-crystallographic two-fold symmetry. (B) Closed-up view of the monomer.

2. Regulation of Enzymatic Activity of a Heme-containing Diguanylate Cyclase (HemDGC) by O_2 Binding to the Heme in the Sensor Domain

Bis-(3',5')-cyclic dimeric guanosine monophosphate (c-di-GMP) is a ubiquitous bacterial second messenger involved in the regulation of cell motility, differentiation, development, virulence, and biofilm formation. This second messenger generally regulates transitions between the free-living, motile lifestyle and the sessile life style. Low concentrations of c-di-GMP promote motile growth, while high concentrations pro-

mote sessile growth with biofilm formation. The intracellular concentrations of c-di-GMP are controlled by the balance between synthesis and hydrolysis of c-di-GMP, which are catalyzed by the enzymes, diguanylate cyclases (DGCs) and phosphodiesterases (PDEs), respectively.

DGCs contain the GGDEF domain, named from the conserved sequence motif (Gly-Gly-Asp-Glu-Phe) that constitutes part of the active site of the enzymes. The GGDEF domain is typically found coupled to a variety of other sensor and/or regulator domains within multidomain proteins.

We have studied the structural and enzymatic properties of a diguanylate cyclase from an obligatory anaerobic bacterium *Desulfotalea psychrophila*, which consists of the N-terminal sensor domain and the C-terminal diguanylate cyclase domain. The sensor domain shows an amino acid sequence homology and spectroscopic properties similar to those of the sensor domains of the globin-coupled sensor proteins containing a protoheme. This heme-containing diguanylate cyclase catalyzes the formation of cyclic di-GMP from GTP only when the heme in the sensor domain binds molecular oxygen. When the heme is in the ferric, deoxy, CO-bound, and NO-bound forms, no enzymatic activity is observed. Resonance Raman spectroscopy reveals that Tyr55 forms a hydrogen bond with the heme-bound O_2 , but not with CO. Instead, Gln81 interacts with the heme-bound CO. These differences of hydrogen bonding network will play a crucial role for the selective O_2 sensing responsible for the regulation of the enzymatic activity.

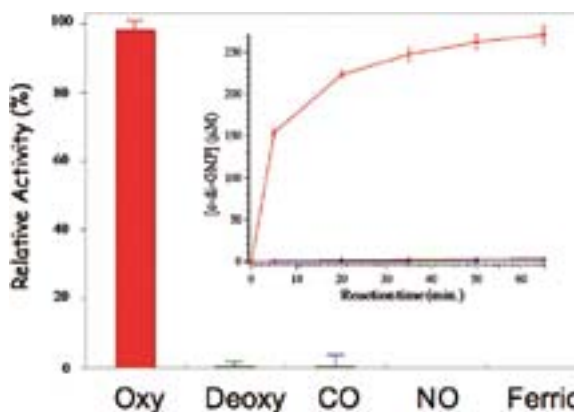


Figure 2. The enzymatic activity of HemDGC is regulated by the coordination state of the heme in its sensor domain. Only when O_2 is bound to the heme, HemDGC shows the activity for the formation of cyclic di-GMP from GTP. Inset: the time-course of the formation of cyclic di-GMP.

Elucidation of the Molecular Mechanisms of Protein Folding

Department of Life and Coordination-Complex Molecular Science
Division of Biomolecular Functions



KUWAJIMA, Kunihiro	Professor
MAKABE, Koki	Assistant Professor
MUKAIYAMA, Atsushi	IMS Fellow
NAKAMURA, Takashi	Post-Doctoral Fellow
CHEN, Jin	Post-Doctoral Fellow
TAKAHASHI, Kazunobu	Graduate Student*
MIZUKI, Hiroko	Technical Fellow
TANAKA, Kei	Secretary

Kuwajima group is studying mechanisms of *in vitro* protein folding and mechanisms of molecular chaperone function. Our goals are to elucidate the physical principles by which a protein organizes its specific native structure from the amino acid sequence. In this year, we studied the folding/unfolding of goat α -lactalbumin, the single-molecule unfolding of staphylococcal nuclease, and the comparative analysis of folding reactions of tear lipocalin and β -lactoglobulin.

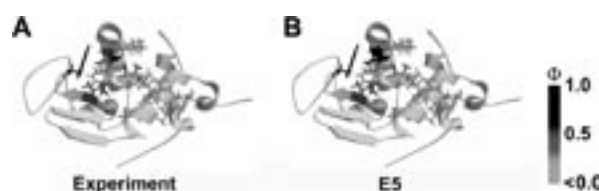


Figure 1. The Φ -values ((a) experimental Φ -values, and (b) Φ_{MD} obtained from molecular dynamics trajectories) mapped onto the three-dimensional structure of goat α -lactalbumin.

1. Experimental and Simulation Studies of the Folding/Unfolding of Goat α -Lactalbumin¹⁾

We studied (1) the unfolding behavior of the authentic and recombinant forms of goat α -lactalbumin and (2) the structure of the transition state of folding/unfolding of the protein, both experimentally and by simulation of the molecular dynamics. Experimentally, the recombinant protein exhibited remarkable destabilization and unfolding-rate acceleration as compared to those of the authentic protein; these differences were caused by the presence of an extra N-terminal methionine residue in the recombinant form. We also characterized the transition state structure by mutational Φ -value analysis, based on which the structure was localized in a region containing the C-helix and the Ca^{2+} -binding site of the protein. Simulation of the molecular dynamics of unfolding at high temperatures (398 and 498 K) yielded good reproduction of the experimental observations and gave atomically detailed descriptions of the unfolding behavior and the transition-state structure of folding/unfolding. The present series thus demonstrated the power of combination of experiments and simulations for studying the problems of protein folding.

2. Probing Force-Induced Unfolding Intermediates of a Single Staphylococcal Nuclease Molecule and the Effect of Ligand Binding²⁾

Single-molecule manipulation techniques have given experimental access to unfolding intermediates of proteins that are inaccessible in conventional experiments. A detailed characterization of the intermediates is a challenging problem that provides new possibilities for directly probing the energy landscape of proteins. We investigated single-molecule mechanical unfolding of a small globular protein, staphylococcal nuclease (SNase), using atomic force microscopy. The unfolding trajectories of the protein displayed sub-molecular and stochastic behavior with typical lengths corresponding to the size of the unfolded substructures. Our results support the view that the single protein unfolds along multiple pathways as suggested in recent theoretical studies. Moreover, we found the drastic change, caused by the ligand and inhibitor bindings, in the mechanical unfolding dynamics.

3. Non-Native α -Helix Formation Is Not Necessary for Folding of Lipocalin: Comparison of Burst-Phase Folding between Tear Lipocalin and β -Lactoglobulin³⁾

Tear lipocalin and β -lactoglobulin are members of the lipocalin superfamily. They have similar tertiary structures but unusually low overall sequence similarity. Non-native helical structures are formed during the early stage of β -lactoglobulin folding. To address whether the non-native helix formation is found in the folding of other lipocalin superfamily proteins, the folding kinetics of a tear lipocalin variant were investigated by stopped-flow methods measuring the time-dependent changes in circular dichroism (CD) spectrum and small-angle X-ray scattering (SAXS). CD spectrum showed that extensive secondary structures are not formed during a burst-phase (within a measurement dead time). The SAXS data showed that the radius of gyration becomes much smaller than in the unfolded state during the burst-phase, indicating that the

molecule is collapsed during an early stage of folding. Therefore, non-native helix formation is not general for folding of all lipocalin family members. The non-native helix content in the burst-phase folding appears to depend on helical propensities of the amino acid sequence.

References

- 1) K. Kuwajima, T. Oroguchi, T. Nakamura, M. Ikeguchi and A. Kidera, in *Water and Biomolecules—Physical Chemistry of Life Phenomena*, K. Kuwajima, Y. Goto, F. Hirata, M. Kataoka and M. Terazima, Eds., Springer-Verlag; Berlin Heidelberg, pp. 13–35 (2009).
- 2) T. Ishii, Y. Murayama, A. Katano, K. Maki, K. Kuwajima and M. Sano, *Biochem. Biophys. Res. Commun.* **375**, 586–591 (2008).
- 3) S. Tsukamoto, T. Yamashita, Y. Yamada, K. Fujiwara, K. Maki, K. Kuwajima, Y. Matsumura, H. Kihara, H. Tsuge and M. Ikeguchi, *Proteins* **76**, 226–236 (2009).

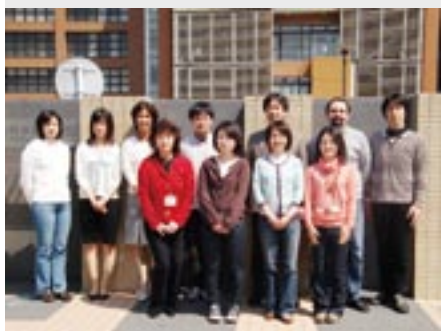
Award

MAKABE, Koki; The Protein Science Society of Japan (PSSJ) Incentive Award for Young Investigators (9th PSSJ Annual Meeting, Kumamoto, May, 2009).

* carrying out graduate research on Cooperative Education Program of IMS with the University of Tokyo

Elucidation of Dynamical Structures of Biomolecules toward Understanding the Mechanisms Underlying Their Functions

Department of Life and Coordination-Complex Molecular Science
Division of Biomolecular Functions



KATO, Koichi
YAMAGUCHI, Takumi
KAMIYA, Yukiko
SERVE, Olivier
SUGIHARA, Takahiro
CHETTERJEE, B. P.
YAGI-UTSUMI, Maho
YOSHIKAWA, Sumi
NISHIO, Miho
YAMAMOTO, Masahiro
BUNKO, Yuji
SUZUKI, Mariko
ISONO, Yukiko
TANAKA, Kei

Professor
Assistant Professor
IMS Research Assistant Professor
Post-Doctoral Fellow
Research Fellow
Visiting Scientist*
Graduate Student†
Graduate Student†
Graduate Student†
Graduate Student†
Graduate Student†
Technical Fellow
Technical Fellow
Secretary

Our biomolecular studies are based on detailed analyses of structures and dynamics of various biological macromolecules and their complexes at atomic level, primarily using nuclear magnetic resonance (NMR) spectroscopy. In particular, we conducted studies aimed at elucidating dynamic structures of glycoconjugates and proteins for integrative understanding of the mechanisms underlying their biological functions. For this purpose, we use multidisciplinary approaches integrating the methodologies of molecular and cellular biology and nano-science along with molecular spectroscopy.

1. Molecular Basis for Glycoprotein-Fate Determination in Cells¹⁻³⁾

Accumulating evidence indicates that a variety of lectins are involved in folding, transport and degradation of glycoproteins in cells. These intracellular lectins are supposed to recognize the *N*-linked oligosaccharides when they act as molecular chaperones, cargo receptors, or ER-associated degradation factors in the quality control system of glycoproteins. To understand the details of the structural and molecular basis of the mechanisms underlying quality control of glycoproteins, we characterize the sugar-binding specificities of the intracellular lectins with a series of intermediates of high-mannose-type oligosaccharides, which are generated through the actions of specific glycosidases in the endoplasmic reticulum. Our frontal affinity chromatographic analyses revealed that molecular chaperone CRT, cargo receptor VIPL, and ER-associated degradation factor OS-9 exhibit distinct sugar-binding specificities (Figure 1). On the basis of these data, we conclude that intracellular lectins recognize distinct 'glycotopes' located on the different site of the high-mannose-type oligosaccharides.

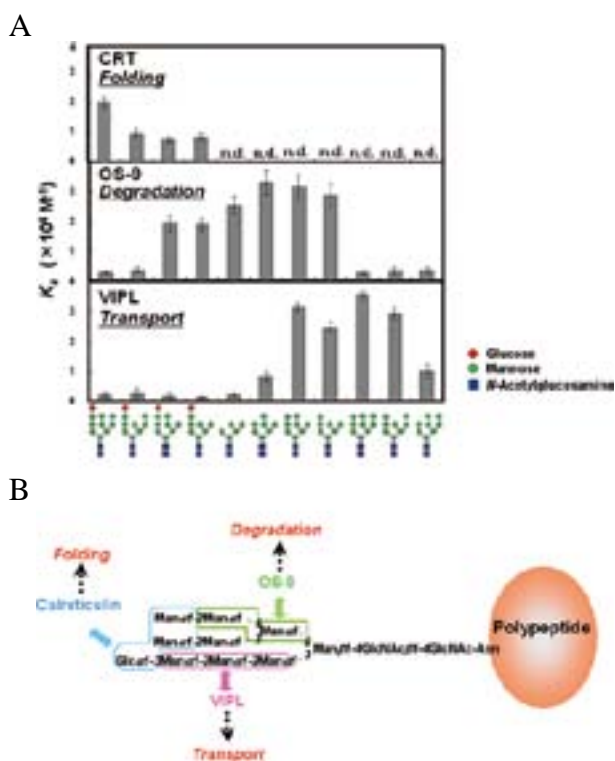


Figure 1. (A) K_a values for CRT, VIPL, and OS-9 determined by the frontal affinity chromatographic analyses. While CRT specifically interacts with monoglucosylated oligosaccharide, VIPL has higher affinity for deglucosylated oligosaccharides. On the other hand, Mannose-trimmed glycans are specifically recognized by OS-9. (B) Schematic representation of a glycoprotein indicating the glycotopes recognized by the intracellular lectins.

2. ^{13}C -Detection NMR Approach for Large Glycoproteins⁴

NMR spectroscopy has great potential to provide us with information on structure and dynamics at atomic resolution of glycoproteins in solution. In larger glycoproteins, however, the detrimental fast ^1H transverse relaxation renders the conventional ^1H -detected NMR experiments difficult. ^{13}C direct detection potentially offers a valuable alternative to ^1H detection to overcome the fast T_2 relaxation. Furthermore, ^{13}C -detected experiments are expected to have several advantages for the NMR spectral assignments of the carbohydrate peaks of glycoproteins. In general, the ^1H signals of glycans except for those originating from the anomeric position are severely overlapped in a narrow spectral region (3–4 ppm) while most ^{13}C signals are dispersed in a wide range (50–110 ppm). Secondly, the information of ^{13}C – ^{13}C shift correlation obtained from the ^{13}C -detected experiments can be helpful in classifying the carbohydrate signals simply by comparing with the reported ^{13}C chemical shift values (Figure 2A). This is due to the fact that ^{13}C chemical shift values of a sugar residue primarily depend on the covalent structures but are not largely affected by the glycosidic linkages conformations and any other environmental factors in contrast to the ^1H chemical shifts, which are influenced, for example, by the interactions with the polypeptide chains. We applied ^{13}C -detected NMR methods to observe the NMR signals of ^{13}C -labeled glycans attached to Fc fragment of immunoglobulin G with a molecular mass of 56 kDa. We successfully demonstrated that ^{13}C -detected ^{13}C – ^{13}C NOESY experiment is highly useful for spectral assignments of the glycans of large glycoproteins because ^{13}C – ^{13}C magnetization transfer is efficiently achieved through dipolar-dipolar interaction in a large glycoprotein due to slower molecular tumbling (Figure 2B). This approach would be in part complementary to ^{13}C – ^{13}C TOCSY and ^1H -detection experiments.

References

- 1) E. M. Quan, Y. Kamiya, D. Kamiya, V. Denic, J. Weibezahn, K. Kato and J. S. Weissman, *Mol. Cell* **32**, 870–877 (2008).
- 2) N. Hosokawa, Y. Kamiya, D. Kamiya, K. Kato and K. Nagata, *J. Biol. Chem.* **284**, 17061–17068 (2009).
- 3) Y. Kamiya, D. Kamiya, R. Urade, T. Suzuki and K. Kato, *Glycobiology Research Trends*, G. Powell and O. McCabe, Eds., NOVA Science Publishers; New York, pp. 27–40 (2009).
- 4) Y. Yamaguchi, M. Wälchli, M. Nagano and K. Kato, *Carbohydr. Res.* **344**, 535–538 (2009).

Award

KAMIYA, Yukiko; Poster Presentation Award, Annual meeting in Protein Community-organization and maintenance of protein functions (2008).

* Present Address; Department of Natural Science, Humanities & Management, West Bengal University of Technology, Kolkata 700-064, India
 † carrying out graduate research on Cooperative Education Program of IMS with Nagoya City University

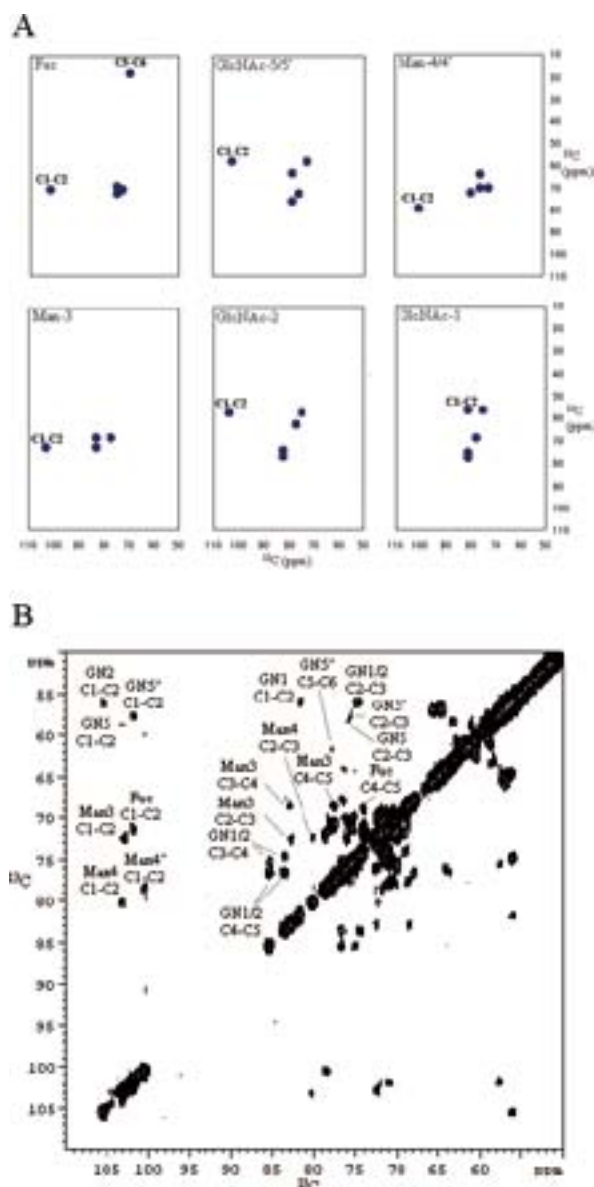
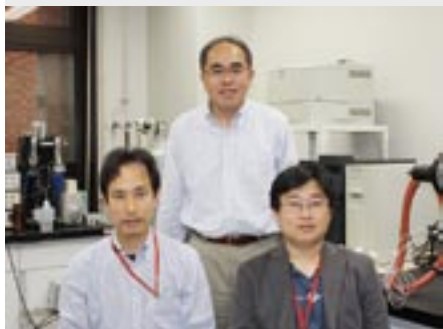


Figure 2. Use of two-dimensional ^{13}C – ^{13}C NOESY spectrum for the assignment of IgG-Fc glycans. (A) Two-dimensional ^{13}C – ^{13}C NOESY patterns expected for the sugar residues, Fuc, GlcNAc-5/5', Man-4/4', Man-3, GlcNAc-2 and GlcNAc-1, in a branched oligosaccharide based on the ^{13}C chemical shift values of the sugar residues in glycopeptides derived from ^{13}C -labeled IgG-Fc. (B) Two-dimensional ^{13}C – ^{13}C NOESY spectrum of ^{13}C -labeled IgG-Fc.

Structure-Function Relationship of Metalloproteins

Department of Life and Coordination-Complex Molecular Science
Division of Biomolecular Functions



FUJII, Hiroshi
KURAHASHI, Takuya
NONAKA, Daisuke
CONG, Zhiqi
TAKAHASHI, Akihiro
TANIZAWA, Misako

Associate Professor
Assistant Professor
IMS Fellow*
IMS Fellow
Graduate Student†
Secretary

Metalloproteins are a class of biologically important macromolecules, which have various functions such as oxygen transport, electron transfer, oxidation, and oxygenation. These diverse functions of metalloproteins have been thought to depend on the ligands from amino acid, coordination structures, and protein structures in immediate vicinity of metal ions. In this project, we are studying the relationship between the electronic structures of the metal active sites and reactivity of metalloproteins.

1. Critical Role of External Axial Ligands in Chirality Amplification of *trans*-Cyclohexane-1,2-diamine in Salen Complexes¹⁾

A series of $\text{Mn}^{\text{IV}}(\text{salen})(\text{L})_2$ complexes bearing different external axial ligands ($\text{L} = \text{Cl}, \text{NO}_3, \text{N}_3$ and OCH_2CF_3) from chiral salen ligands with *trans*-cyclohexane-1,2-diamine as a chiral scaffold are synthesized, in order to gain insight into conformational properties of metal salen complexes. X-ray crystal structures show that $\text{Mn}^{\text{IV}}(\text{salen})(\text{OCH}_2\text{CF}_3)_2$ and $\text{Mn}^{\text{IV}}(\text{salen})(\text{N}_3)_2$ adopt a stepped conformation with one of two salicylidene rings pointing upward and the other pointing downward due to the bias from the *trans*-cyclohexane-1,2-diamine moiety, which is in clear contrast to a relatively planar solid-state conformation for $\text{Mn}^{\text{IV}}(\text{salen})(\text{Cl})_2$. The CH_2Cl_2 solution of $\text{Mn}^{\text{IV}}(\text{salen})(\text{L})_2$ shows circular dichroism of increasing intensity in the order of $\text{L} = \text{Cl} < \text{NO}_3 < \text{N}_3 < \text{OCH}_2\text{CF}_3$, which indicates $\text{Mn}^{\text{IV}}(\text{salen})(\text{L})_2$ adopts a solution conformation of an increasing chiral distortion in this order. Quantum-chemical calculations with symmetry adapted cluster–configuration interaction method indicate that a stepped conformation exhibits more intense circular dichroism than a

planar conformation. The present study clarifies an unexpected new finding that the external axial ligands (L) play a critical role in amplifying the chirality in *trans*-cyclohexane-1,2-diamine in $\text{Mn}^{\text{IV}}(\text{salen})(\text{L})_2$ to facilitate the formation of a chirally-distorted conformation, possibly a stepped conformation.

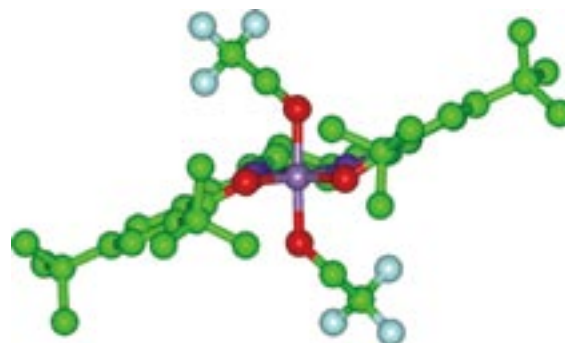


Figure 1. Chiral stepped conformation of $\text{Mn}^{\text{IV}}(\text{salen})(\text{OCH}_2\text{CF}_3)_2$.

2. Catalytic Reactivity of a *Meso*-N-Substituted Corrole and Evidence for a High-Valent Iron–Oxo Species²⁾

It is shown that an iron(III) *meso*-N-substituted corrole ($\text{TBP}_8\text{Cz})\text{Fe}^{\text{III}}$ (**1**) (TBP_8Cz) octakis(4-*tert*-butylphenyl)corrol azinato), is a potent catalyst for the oxidation of alkenes in the presence of pentafluoroiodosylbenzene ($\text{C}_6\text{F}_5\text{IO}$) as oxidant. In the case of cyclohexene, complex **1** performs on a par with one of the best porphyrin catalysts ((TPPF_{20}) FeCl), exhibiting rapid turnover and a high selectivity for epoxide ($\text{CzFe}^{\text{III}}/\text{C}_6\text{F}_5\text{IO}/\text{cyclohexene}$ (1:100:1000) in $\text{CH}_2\text{Cl}_2/\text{CH}_3\text{OH}$ (3:1 v: v) gives 33 turnovers of epoxide in <2 min). Reaction rates for **1** are greatly enhanced compared to other Fe or Mn corroles

under similar catalytic conditions, consistent with an increase in the electrophilicity of a high-valent iron-oxo intermediate induced by *meso-N* substitution. Reaction of dark-green **1** (λ_{max} 440, 611, 747 nm) under single-turnoverlike conditions at -78 °C leads to the formation of a new dark-brown species (**2**) (λ_{max} 396, 732, 843 nm). The Fe^{III} complex **1** is restored upon the addition of 2 equiv of ferrocene to **2**, or by the addition of 1 equiv of PPh₃, which concomitantly yields OPhP₃. In addition, complex **2** reacts with excess cyclohexene at -42 °C to give **1**. Complex **2** was also characterized by EPR spectroscopy, and all of the data are consistent with **2** being an antiferromagnetically coupled iron(IV)-oxo π -cation-radical complex. Rapidmixing stopped-flow UV-vis studies show that the low-temperature complex **2** is generated as a shortlived intermediate at room temperature.

3. Effect of Imidazole and Phenolate Axial Ligands on the Electronic Structure and Reactivity of Oxoiron(IV) Porphyrin π -Cation Radical Complexes: Drastic Increase in Oxo-Transfer and Hydrogen Abstraction Reactivities³⁾

To study the effect of axial ligands on the electronic structure and reactivity of compound I of peroxidases and catalases, oxoiron(IV) porphyrin π -cation radical complexes with imidazole, 2-methylimidazole, 4(5)-methylimidazole, and 3-fluoro-4-nitrophenolate as the axial ligands were prepared by ozone oxidation of iron(III) complexes of 5, 10, 15, 20-tetramesitylporphyrin (TMP) and 2, 7, 12, 17-tetramethyl-3, 8, 13, 18-tetramesitylporphyrin (TMTMP). These complexes were fully characterized by absorption, ¹H, ²H, and ¹⁹F NMR, EPR, and ESI-MS spectroscopy. The characteristic absorption peak of compound I at approximately 650 nm was found to be a good marker for estimation of the electron donor effect from the axial ligand. The axial ligand effect did not change the porphyrin π -cation radical state, the a_{2u} state of the TMP complexes, or the a_{1u} radical state³⁾ of both the TMTMP complexes and compound I. The ferryl iron and porphyrin π -cation radical spins were effectively transferred into the axial ligands for the a_{2u} complexes, but not for the a_{1u} complexes. Most importantly, the reactivity of the oxoiron(IV) porphyrin π -cation radical complex was drastically increased by the imidazole and phenolate axial ligands. The reaction rate for cyclooctene epoxidation was increased 100 ~ 400-fold with axial coordination of imidazoles and phenolate. A similar increase was also observed for oxidation of 1,4-cyclohexadiene, *N,N*-dimethyl-*p*-nitroaniline, and hydrogen peroxide. These results suggest extreme enhancement of the reactivity of compound I by the axial ligand in heme enzymes. The functional role of axial ligands on the compound I in heme enzymes is discussed.

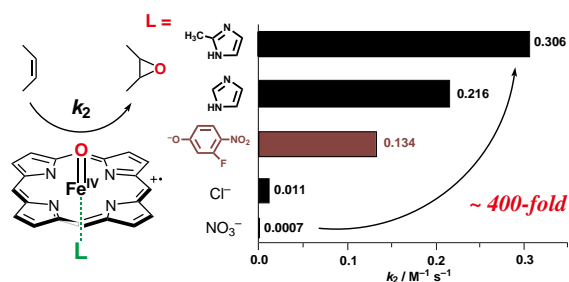


Figure 2. Axial ligand effect on the epoxidation reactivity.

4. Paramagnetic ¹³C and ¹⁵N NMR Analyses of Cyanide (¹³C¹⁵N)-Ligated Ferric Peroxidases: The Push-Effect, not Pull-Effect, Modulates the Compound I Formation Rate⁴⁾

Paramagnetic ¹³C and ¹⁵N NMR spectroscopy of heme-bound cyanide (¹³C¹⁵N) was utilized to quantitatively distinguish the electron donor effect (the push-effect) from the proximal histidine and hydrogen bonding effect (the pull-effect) from the distal amino acid residues in cytochrome *c* peroxidase (CcP), ascorbate peroxidase (APX), lignin peroxidase (LiP) and manganese peroxidase (MnP). Paramagnetic ¹³C NMR signals of heme-bound ¹³C¹⁵N of these peroxidases were observed in a wide range: -3501 ppm (CcP), -3563 ppm (APX), -3823 ppm (MnP), and -3826 ppm (LiP), while paramagnetic ¹⁵N NMR signals of those were detected in a narrow range: 574 ppm (ARP), 605 ppm (CcP), 626 ppm (LiP), and 654 ppm (MnP). Detailed analysis, combined with the previous results for horseradish peroxidase and *Arthromyces ramosus* peroxidase, indicated that the push-effect is quite different among these peroxidases while the pull-effect is similar. More importantly, a strong correlation between the ¹³C NMR shift (the push-effect) and the compound I formation rate was observed, indicating that the push-effect causes a variation in the compound I formation rate. Comparison of the ¹³C and ¹⁵N NMR results of these peroxidases with their crystal structures suggests that the orientation of the proximal imidazole plane to the heme N-Fe-N axis controls the push-effect and the compound I formation rate of peroxidase.

References

- 1) T. Kurahashi, M. Hada and H. Fujii, *J. Am. Chem. Soc.* in press.
- 2) A. J. McGrown, W. D. Kerber, H. Fujii and D. P. Goldberg, *J. Am. Chem. Soc.* **131**, 8040–8048 (2009).
- 3) A. Takahashi, T. Kurahashi and H. Fujii, *Inorg. Chem.* **48**, 2614–2625 (2009).
- 4) D. Nonaka, H. Wariishi and H. Fujii, *Biochemistry* **48**, 898–905 (2009).

* Present Address; Osaka University, Suita, Osaka 565-0871

† Present Address; Sumika Chemical Analysis Service, Ltd. Osaka 541-0043

Fabrication of Silicon-Based Planar Ion-Channel Biosensors and Integration of Functional Cell Membrane Model Systems on Solid Substrates

Department of Life and Coordination-Complex Molecular Science
Division of Biomolecular Sensing



URISU, Tsuneo
YANG, Dah-Yen
TERO, Ryugo
ASANO, Toshifumi
NAGAIRO Takeshi
UNO, Hidetaka
NAKAI, Naohito
SHANG, Zhi-Guo
FUJIWARA, Kuniyo
SAYED, Abu
HE, Tingchao
SHIMIZU, Atsuko

Professor
Visiting Professor
Assistant Professor
IMS Fellow
Research Fellow
Graduate Student
Graduate Student
Graduate Student
Graduate Student
Graduate Student*
Secretary

We are interested in the investigation of cell membrane surface reactions and the pathogen mechanism of the neurodegenerative diseases, based on the molecular science. We are advancing two subjects, aiming the creation and development of new molecular science field, “medical molecular science.” One is the development of ion channel biosensor and its application to the neural network analyzer device. The other is the fundamental understanding of bilayer membrane properties using the artificial lipid bilayers on solid substrates, which is called supported bilayers, by means of atomic force microscope and fluorescence microscope-based techniques.

1. Development of Cell-Culture-Type Planar Ion Channel Biosensor¹⁾

We have developed a new planar-type ion channel biosensor with a silicon-on-insulator (SOI) substrate and a cell culture function. Fibronectin is coated on the substrate surface to promote cell growth in this sensor. A transient receptor potential vanilloid type 1 (TRPV1) channel-expressing HEK293 cell is

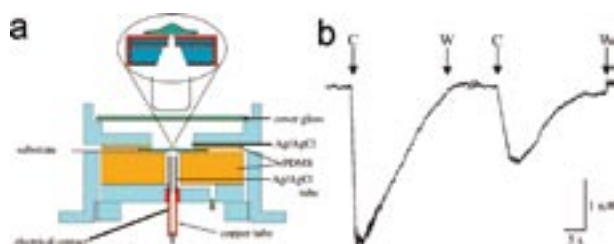


Figure 1. (a) Schematic drawing of the incubation-type planar ion channel biosensor. The sensor chip is fabricated using Si-SOI substrates ($7 \times 7 \text{ mm}^2$) with micropores at the center. (b) Whole-cell channel current recording of TRPV1-transfected HEK-293; current was activated by repeated capsaicin stimulation (c) and wash-out (w) cycles.

positioned on the micropore of the SOI sensor chip and incubated. Although the seal resistance was quite small, $10\text{--}20 \text{ M}\Omega$, compared with that of the conventional pipette patch-clamp method, the signal-to-noise level was sufficiently high. However, a much lower noise level is required for observing the opening and closing of fewer than 30 channels.

2. Noise Properties of Incubation-Type Planar Ion Channel Biosensor²⁾

Noise properties are the most important issues in the planar-type ion channel biosensors, as well as in the pipette patch-clamp and black membrane biosensors. Therefore the current noise and its power spectrum appearing in the incubation-type planar ion channel biosensor (Figure 1) were

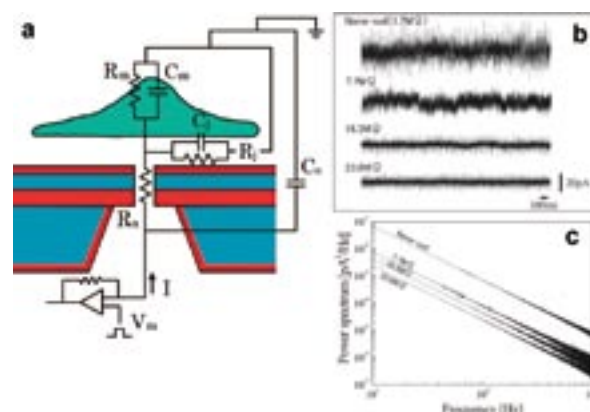


Figure 2. (a) Equivalent circuit of the incubation-type planar ion channel biosensor. The oxide layer of SOI and the $\sim 1\text{-}\mu\text{m}$ -thick surface oxide layer are important for reducing substrate capacitance C_s . (b, c) Observed noise properties of the incubation -type planar ion channel biosensor: (b) noise current and (c) its spectral density for various cleft resistances (R_i).

measured and analyzed in detail to detect the main origin of the noise. The dominant noise sources are classified into (i) current noise induced by head stage preamplifier input voltage noise, (ii) thermal noise, and (iii) excess noise. The spectral density and variance of these noises are formulated in the general form using an equivalent circuit shown in Figure 2a. The baseline currents at various cleft resistance (R_j in Figure 2a) were measured (Figure 2b) and their power spectra were calculated (Figure 2c). We concluded that the main source of the noise in the device is the excess noise, which depends on $1/f$ and originates primarily from the current passing through the cleft between the cell membrane and the substrate surface. The measured noise level ($1.0\text{--}2.4 \times 10^{-11}$ A) corresponds to channel current through 5–10 membrane proteins, thus sufficiently small to measure the signal of whole-cell current ($\sim 10^{-9}$ A) (Figure 1b).

3. Synchrotron-Radiation-Stimulated Etching of Polydimethylsiloxane (PDMS) Using XeF_2 as a Reaction Gas³⁾

The synchrotron radiation (SR) stimulated etching of silicon elastomer polydimethylsiloxane (PDMS) using XeF_2 as an etching gas has been demonstrated. The etching system with differential pumps and two parabolic focussing mirrors was constructed to perform the etching. The PDMS was found to be effectively etched by the SR irradiation under the XeF_2 gas flow, and the etching process was area-selective and anisotropic. Extremely high etching rate of 40–50 μm was easily obtained at the XeF_2 gas pressure of 0.2–0.4 Torr. This suggests that SR etching using XeF_2 gas provides a new microfabrication technology for thick PDMS membranes, which can open new applications such as the formation of three dimensional microfluidic circuits.

4. Surface-Induced Phase Separation of Sphingomyelin/Cholesterol/Ganglioside GM1-Planar Bilayer on Mica Surfaces and Molecular Conformation that Accelerates $\text{A}\beta$ Oligomerization

Lipid bilayers containing ganglioside GM1 (GM1) are used in the development of new therapies for Alzheimer's disease (AD), because GM1 mediates the amyloid beta ($\text{A}\beta$) aggregation that is the hallmark of AD. To investigate how ganglioside-containing lipid bilayers interact with $\text{A}\beta$, we examined the interaction between $\text{A}\beta_{40}$ and supported planar lipid bilayers (SPLBs) on mica and SiO_2 substrates using

atomic force microscopy, fluorescence microscopy, and molecular dynamics computer simulations. These SPLBs contained several compositions of sphingomyelin, cholesterol, and GM1 which covers compositions commonly seen in eukaryotic biomembranes and were treated at physiological salt concentrations. Surprisingly high speed $\text{A}\beta$ aggregations of fibril formation were induced for all GM1 concentrations examined on the mica surface, but only globular agglomerates are formed slowly on the SiO_2 surfaces. Especially for the 20 mol% GM1 concentration on the mica surface, unique triangular domains were formed and the high speed $\text{A}\beta$ aggregations were observed only outside of the triangular domains. The speed of $\text{A}\beta_{40}$ aggregation and the shape of the agglomerates depend on the molecular conformation of GM1, which varies depending on the substrate materials.

5. Shape Transformation of Adsorbed Vesicles on Oxide Surfaces: Effect of Substrate Material and Photo-Irradiation⁴⁾

Shape transformation of phospholipid vesicles on oxide surfaces was investigated by a fluorescence microscope. The transformation of spherical vesicles to a planar lipid bilayer membrane spontaneously proceeded on mica and glass, while the intact vesicular layer formed on TiO_2 . Interaction energy between the substrate and the bilayer, which was evaluated using the rigorously calculated Hamaker constant, was ~ 10 times larger on TiO_2 than on mica and SiO_2 . The results seem inconsistent with the conventionally proposed adhesion induced tension model, in which stronger adsorption leads to easier planar membrane formation from vesicles, thus indicate that the shape transformation from vesicles to a planar membrane is dominated by the kinetic processes and the dynamics of the vesicles, rather than the adsorption state of individual vesicle. Area-selective SPLB formation of adsorbed vesicles was induced by the irradiation of strong excitation light, which was assisted by the photo-induced expansion of SPLB containing dye-labeled lipid molecules.

References

- 1) T. Asano, H. Uno, K. Shibasaki, M. Tominaga and T. Urisu, *Trans. Mater. Res. Soc. Jpn.* **33**, 767–770 (2008).
- 2) T. Asano, T. Nakamura, A. Wakahara and T. Urisu, *Jpn. J. Appl. Phys.* **48**, 027001 (4 pages) (2009).
- 3) T. -Y. Chiang, T. Makimura, T. He, S. Torii, R. Tero, C. Wand and T. Urisu, *Rev. Sci. Instrum.* **17**, 69–74 (2010).
- 4) R. Tero, T. Ujihara and T. Urisu, *Trans. Mater. Res. Soc. Jpn.* **34**, 183–188 (2009).

Awards

ASANO, Toshifumi; The best poster award in 2nd International Symposium on Nanomedicine.

TERO, Ryugo; The best poster award in 61th Divisional Meeting on Colloid and Interface Chemistry, CSJ.

* from Shanghai Jiao Tong University

Investigation of Molecular Mechanisms of Transporters and Receptors in Membrane by Using Stimulus-Induced Difference FT-IR Spectroscopy

Department of Life and Coordination-Complex Molecular Science
Division of Biomolecular Sensing



FURUTANI, Yuji
SHIMIZU, Atsuko

Associate Professor
Secretary

The cell, the elementary unit of life, uptakes nutrient and exhausts waste. Its ion balance between inside and outside of cell membrane is adjusted strictly. These works are performed by membrane proteins such as channels and transporters. There are some other membrane proteins such as cell sensor proteins which detect various environmental changes. A main goal of my group is to clarify molecular mechanisms of transporters and receptors in cell membrane mainly by using stimulus-induced difference infrared spectroscopy which is sensitive to structural and environmental changes of protein molecules.

I have moved to IMS in this March and have been setting up my lab. In this review article, I'd like to present my recent studies done in my previous work place, Nagoya Institute of Technology, and progress in a recent research by using a new FT-IR spectrometer installed in IMS.

1. Time-Resolved FT-IR Spectroscopy Detecting O–H and O–D Stretching Vibrations of Internal Water Molecules in a Light-Driven Proton Pump Protein, Bacteriorhodopsin

Bacteriorhodopsin (bR) is one of well known light-driven proton pump protein, which has an all-*trans* retinal covalently linked to Lys216 via a protonated Schiff base (SB). Upon light absorption, photo-isomerization occurs from the all-*trans* to 13-*cis* form in less than one picosecond, followed by a cyclic reaction that comprises a series of intermediates, called as the K, L, M, N, and O states, back to the bR ground state (BR). During the bR photocycle the first proton transfer reaction takes place in the L to M transition. A proton is transferred

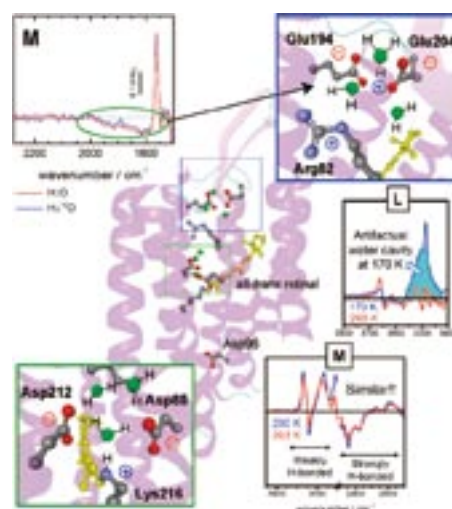


Figure 1. X-ray crystal structure of bacteriorhodopsin and O–H stretching vibrations observed in its photocycle. Several water molecules exist in the protein cavities and play an important role for pumping protons.

from the protonated SB to Asp85, together with the apparently simultaneous release of a proton from the so-called proton release group (PRG), which is composed of water molecules, Glu194 and Glu204, to the extracellular side. Further proton transfers take place in the later intermediates (accompanied by other protein and retinal structural changes), leading to a net proton transport from the cytoplasmic to the extracellular side, and the recovery of the bR ground state.

By use of time-resolved FT-IR spectroscopy with bR film samples moderately hydrated with water, H₂O, or isotope labeled water, H₂¹⁸O, infrared difference spectra in O–H

stretching region were successfully collected and some of the bands were assigned to the internal water molecules (Figure 1). Especially, we firstly gave experimental evidence that the continuum band in the 2000–1800 cm^{-1} region was originated from the protonated water cluster which probably locates in the extracellular side.¹⁾ It was also elucidated that water structure formed in the L intermediate at room temperature is different from that trapped in low temperature.

Now, I try to extend observable spectral range to the region around peak of water absorption, 3400 cm^{-1} in H_2O and 2400 cm^{-1} in D_2O . By use of D_2O and optimizing hydration level, accurate light-induced difference spectra were collected (Figure 2). In the X–H and X–D stretching region, structural changes in the hydrophobic and hydrophilic part were separately observed, respectively. By analyzing these spectral changes, real-time hydrogen-bonding changes of the internal water molecules and protein moiety of bR will be elucidated, leading to better understand of the light-driven proton pumping mechanism of bR.

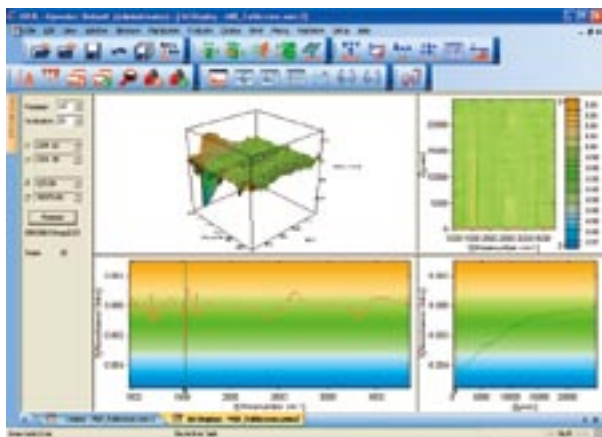


Figure 2. Time-resolved FT-IR spectra of bacteriorhodopsin in the whole mid-infrared region. By use of D_2O and optimizing hydration level, plausible spectral changes were observed.

2. Perfusion-Induced Difference FT-IR Spectroscopy Investigating Ion Binding Sites of Membrane Proteins

Membrane proteins are important for homeostasis of living cells, which work as ion channel, ion pump, various types of chemical and biophysical sensors, *etc.* These proteins are considered as one of important targets for biophysical studies. However, their molecular mechanisms have not been studied well, because X-ray crystallography and NMR spectroscopy are hard to access them in general. Recently, it has been demonstrated that stimulus-induced attenuated total reflection (ATR) FTIR spectroscopy is another promising technique for investigating molecular mechanism of membrane proteins.

In 2009 before coming to IMS, I have demonstrated molecular mechanism of the proton releasing group (PRG) in

pharaonis phoborhodopsin (ppR) by means of Cl^- -induced and light-induced difference ATR-FTIR spectroscopy in aqueous condition.²⁾ *Pharaonis* phoborhodopsin (ppR, also called *pharaonis* sensory rhodopsin II; pSRII) is a photoreceptor for negative phototaxis in *Natronomonas pharaonis*, and in the absence of transducer protein, pHtrII, ppR can pump protons like BR. Fast, BR-like proton release was observed during the lifetime of the M intermediate (ppR_M) at acidic pH, but it was diminished in the absence of Cl^- . It was suggested that Cl^- binding controls the pKa of PRG in ppR and ppR_M.

As shown in Figure 3, Cl^- -induced difference ATR-FTIR spectra clearly demonstrated that Cl^- -binding to ppR accompanies protonation of a carboxylic acid (C=O stretch at 1724 cm^{-1}). The amino acid was identified as Asp193, because the corresponding band is shifted to 1705 cm^{-1} in the D193E mutant protein. It means that the PRG of ppR includes Asp193, whose pKa change is partly controlled by Cl^- .

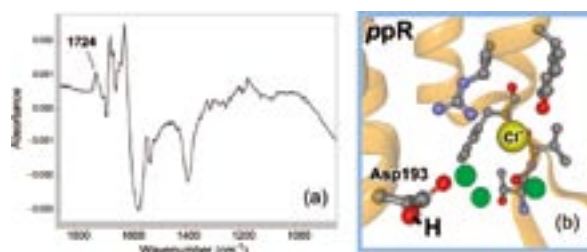


Figure 3. (a) Chloride-ion binding induced difference infrared spectra of a membrane protein (*pharaonis* phoborhodopsin; light sensor in an archaeobacterium). The 1724- cm^{-1} band was assigned to the protonated carboxylate group of Asp193. (b) The existence of hydrogen at Asp193, which has not been detected by X-ray crystallography, was revealed by infrared spectroscopy.

Application of ATR-FTIR to other membrane proteins, such as an ion channel (KcsA) and a transporter protein (V-ATPase), started before coming to IMS. It has been succeeded to measure the difference infrared spectra between the conditions of several types of ions and pH. Based on these spectra, the molecular mechanism of recognition and transportation of ions will be discussed in the near future.

At IMS, I will develop new methods of stimulus-induced ATR-FTIR spectroscopy by constructing stopped-flow system or using caged compounds for improving time-resolution. Reduction of buffer waste is also important for using isotope labeled water or expensive reagents, which will be achieved by designing a micro-flow chamber.

References

- 1) V. A. Lórenz-Fonfría, Y. Furutani and H. Kandori, *Biochemistry* **47**, 4071–4081 (2008).
- 2) Y. Kitade, Y. Furutani, N. Kamo and H. Kandori, *Biochemistry* **48**, 1596–1603 (2009).

Heterogeneous Catalytic Systems for Organic Chemical Transformations in Water

Department of Life and Coordination-Complex Molecular Science
Division of Complex Catalysis



UOZUMI, Yasuhiro
OSAKO, Takao
HAMASAKA, Go
MATSUURA, Yutaka
YAMAMOTO, Yoshikazu
HIRAI, Yoshinori
BEPPU, Tomohiko
WATANABE, Toshihiro
KOBAYASHI, Noboru
MUTO, Tsubasa
TORII, Kaoru
SASAKI, Tokiyo
TANIWAKE, Mayuko
FUKUSHIMA, Tomoko

Professor
Assistant Professor
Post-Doctoral Fellow
Post-Doctoral Fellow
Post-Doctoral Fellow
Research Fellow
Graduate Student
Graduate Student
Graduate Student
Graduate Student
Technical Fellow
Secretary
Secretary
Secretary

Various organic molecular transformations catalyzed by transition metals were achieved under heterogeneous aqueous conditions by use of amphiphilic resin-supported metal complexes or convoluted polymeric metal catalysts which were designed and prepared by this research group. In particular, asymmetric Suzuki-Miyaura coupling and oxidative cyclization of alkenols and alkenoic acids, both of which were performed in water under heterogeneous conditions with high recyclability of the polymeric catalysts, are highlights among the achievements of the 2008–2009 period to approach what may be considered ideal chemical processes of next generation. Representative results are summarized hereunder.

1. Synthesis of [2,6-Bis(2-oxazoliny)phenyl]palladium Complexes via the Ligand Introduction Route¹⁾

A series of [2,6-bis(2-oxazoliny)phenyl]palladium (Phebox-Pd) complexes were synthesized via the ligand introduction route. *trans*-Bromo(2,6-dicarboxyphenyl)bis(triphenyl phosphine)palladium was prepared by the reaction of 2-bromoisophthalic acid with Pd(PPh₃)₄ in 93% yield, and the

carboxy groups of the palladium complex were converted into the oxazoliny groups to give the Phebox-Pd complexes in 44–57% yield (Scheme 1).

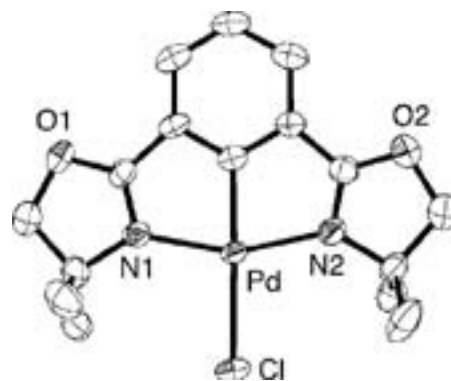
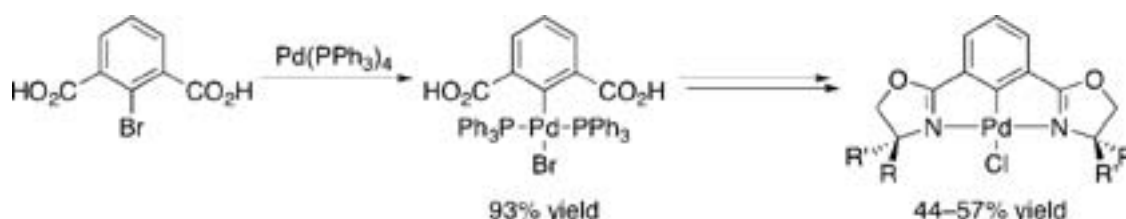


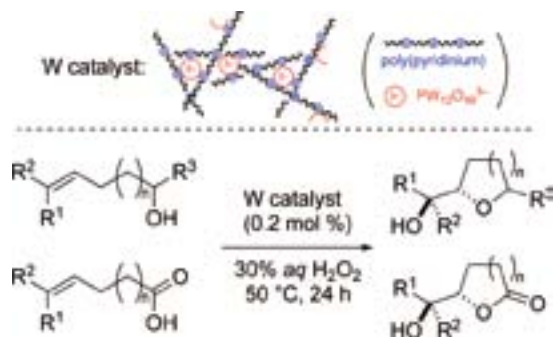
Figure 1. ORTEP drawing of Phebox-Pd complex.



Scheme 1. Ligand Introduction Route for the Synthesis of [2,6-Bis(2-oxazoliny)phenyl]palladium Complexes.

2. Development of Tightly Convolved Polymeric Phosphotungstate Catalysts and Their Application to an Oxidative Cyclization of Alkenols and Alkenoic Acids²⁾

Tightly convoluted polymeric phosphotungstate catalysts were prepared via ionic-assembly of $\text{H}_3\text{PW}_{12}\text{O}_{40}$ and poly(alkylpyridinium)s. An oxidative cyclization of various alkenols and alkenoic acids was efficiently promoted by the polymeric phosphotungstate catalyst in *aq.* H_2O_2 in the absence of organic solvents to afford the corresponding cyclic ethers and lactones in high yield. The catalyst was reused four times without loss of catalytic activity. The polymeric phosphotungstate was unambiguously characterized by spectro- and microscopic studies (MAS $^{31}\text{P}\{^1\text{H}\}$ NMR, IR spectroscopy, elemental analysis, TEM, SEM, and EDS).



Scheme 2. Oxidative Cyclization of Alkenyl Alcohols and Alkenoic Acids with a Convolved Polymeric Phosphotungstate.

3. Asymmetric Suzuki-Miyaura Coupling in Water with an Amphiphilic Resin-Supported Chiral Palladium Catalyst³⁾

Asymmetric Suzuki-Miyaura coupling of aryl halides (Cl, Br, I) and aryl boronic acids was achieved in water with wide functional group tolerance by use of a readily-recyclable amphiphilic polymer (PS-PEG) resin-supported chiral imidazoindolephosphine-palladium complex to give a variety of biaryls with up to 94 % ee.



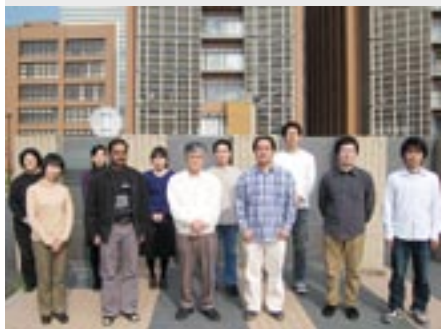
Scheme 3. Asymmetric Suzuki-Miyaura Coupling in Water with an Amphiphilic Resin-Supported Chiral Palladium Complex.

References

- 1) T. Kimura and Y. Uozumi, *Organometallics* **27**, 5159–5162 (2008).
- 2) Y. M. A. Yamada, H. Guo and Y. Uozumi, *Heterocycles* **76**, 645–655 (2008).
- 3) Y. Uozumi, Y. Matuura, T. Arakawa and Y. M. A. Yamada, *Angew. Chem., Int. Ed.* **48**, 2708–2710 (2009).

Synthesis of Metal Complexes Aiming at Reversible Conversion between Chemical Energy and Electrical One

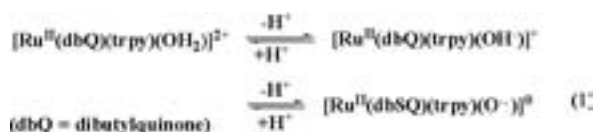
Department of Life and Coordination-Complex Molecular Science
Division of Functional Coordination Chemistry



TANAKA, Koji
WADA, Tohru
OHTSU, Hideki
FUKUSHIMA, Takashi
SUMANTA, Kumar
BAI, Zhengshuai
MIYAJI, Mariko
TSUKAHARA, Yuhei
YAMAGUCHI, Yumiko
NAKAGAKI, Shizuka

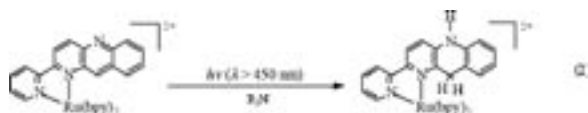
Professor
Assistant Professor
IMS Research Assistant Professor
Post-Doctoral Fellow
Post-Doctoral Fellow
Post-Doctoral Fellow
Post-Doctoral Fellow
Graduate Student
Secretary
Secretary

Metal ions involved in various metal proteins play key roles to generate metabolic energies through redox reactions of bio-organic molecules. Metal complexes that have an ability to oxidize organic molecules at potentials more negative than reduction of dioxygen are feasible molecular energy converters from chemical energy to electrical one. High valent Ru=O complexes are prepared by sequential proton and electron loss of the correspondent aqua-Ru complexes. Although some of them are active for the oxidation of organic molecules, the oxidation potentials required to convert from Ru-OH₂ to high valent Ru=O species are generally too positive for the purpose of the use as the energy converters. On the other hand, unusual Ru-oxyl radical complexes spontaneously are formed by deprotonation of aqua-Ru-dioxolene complexes due to intramolecular charge transfer from the negatively charged deprotonated aqua ligand to dioxolene (eq 1). Oxyl radical



complexes formed in eq 1 are expected to have an ability to abstract hydrogen atom of C-H bonds of organic molecules, which would play the key role in the energy conversion from chemical energy to electrical one.

The difficulty in photochemical activation of small inorganic molecules such as N₂, O₂, CO₂, and H₂O results from the undesirable formation of high energy intermediates that are produced by stepwise one-electron transfer to the reaction centers. Recently, we showed that a mononuclear [Ru^{II}(pbn)(bpy)₂]²⁺ (bpy = 2,2'-bipyridine, pbn = 2-(2-pyridyl)benzo[*b*-



1,5-naphthyridine) ([1]²⁺) is smoothly reduced to [Ru(pbnH₂)(bpy)₂]²⁺ ([1H₂]²⁺) under visible light irradiation in the presence of sacrificial electron donors (eq 2). Furthermore, oxidation of [1H₂]²⁺ by appropriate oxidants smoothly regenerates [1]²⁺. Thus, the [1H₂]²⁺/[1]²⁺ redox couple is the first functional model of the nicotinamide adenine dinucleotide NAD⁺/NADH redox reaction that works as a reservoir/source of two electrons and one proton in various biological energy transfer systems.

1. Synthesis and Electrochemical Reduction of Novel Ruthenium Complex Having *N,N*-Bis(benzo[*b*]-1,5-naphthyridin-2-ylmethyl)propane-2-amine Ligand as NAD⁺/NADH Type Redox Site

Hydrogenation is one of the most important reactions in chemical transformations of a wide range of materials. A variety of metal-hydrides have been used in catalytic hydrogenation reactions under hydrogen gas, but those compounds are generally sensitive to water because of their high reactivity. Alternatively, electrocatalytic reduction without using hydrogen gas has several advantages such as clean, simple, safe, and easy regulation of reactivity of catalysts by choosing applied potentials. On the other hand, the nicotinamide adenine dinucleotide redox couple (NAD⁺/NADH) functions as a reservoir/source of two electrons and one proton in various biological redox reactions. To mimic the efficiency and versatility of the NAD⁺/NADH redox couple, a variety of model reactions have been conducted by using NADH model compounds. However, the reactions reported so far have been limited to stoichiometric ones. We, therefore, prepared [Ru(bpy)₂(pbn)](PF₆)₂ as a molecular electrocatalyst to simulate the function of the NAD⁺/NADH redox couple. As mentioned above, the [Ru(bpy)₂(pbn)]²⁺/[Ru(bpy)₂(pbnH₂)]²⁺ redox couple well simulates the NAD⁺/NADH couple. To improve the ability of

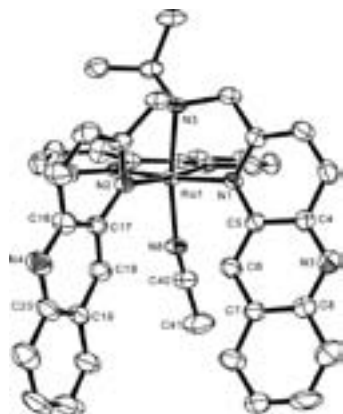
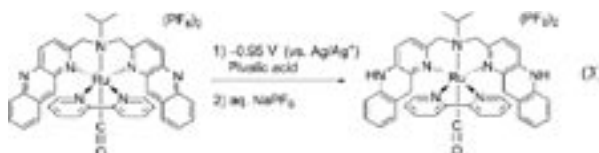


Figure 1. Crystal structure of $[\text{Ru}(\text{bbnma})(\text{CH}_3\text{CN})]^{2+}$.

multi-electron redox reaction of pbn, a new type of tridentate ligand, *N,N*-bis(benzo[*b*]-1,5-naphthyridin-2-ylmethyl) propane-2-amine (denoted as bbnma) possessing two benzo[*b*]-1,5-naphthyridines tethered to tertiary amine was designed and its ruthenium complex, $[\text{Ru}(\text{bbnma})(\text{bpy})\text{L}](\text{PF}_6)_2$, was synthesized. The conception of bbnma is to make a space not only to introduce substrates (*e.g.* ketones, imines, and related substrates) into the ruthenium center by a substitution reaction but also to place them forcibly at the vicinity of the two NADH type hydride sources generating on bbnma coordinated in a facial fashion (Figure 1). In fact, $[\text{Ru}(\text{bbnma})(\text{bpy})(\text{CO})]^{2+}$ smoothly underwent four-electron reduction under the electrolysis at -0.95 V in the presence of pivalic acid, and $[\text{Ru}(\text{bbnmaH}_4)(\text{bpy})(\text{CO})]^{2+}$ was obtained in a high yield.



2. Photoinduced Four-, and Six-Electron Reduction of Mononuclear Ruthenium Complexes Bearing NAD⁺ Analogous Ligands

The development of artificial photosynthetic processes aiming to generate high-energy molecules from low-energy ones (*e.g.* reduction of carbon dioxide or water splitting) is the top research priority to regulate consumption of non-renewable fossil fuels against the strong pressure of the energy demand that keeps increasing. Multi-electron reactions through stepwise one-electron transfer inevitably generate high-energy free radical intermediates, which often yield undesired products. Therefore construction of artificial photosynthetic systems that are able to mediate multi-electron transfer from photosensitizers to the reaction sites without accompanying high energy intermediates would open new era to achieve light-driven multi-electron carbon dioxide reduction and water splitting.

Despite the large efforts devoted to the development of complex supramolecular assemblies for light harvesting and directional charge separation, photosynthetic systems designed for light-induced multi-electron transfer rarely generate reducing equivalents. As mentioned above, we have succeeded photochemical two-electron reduction of $[\text{Ru}(\text{bpy})_2(\text{pbn})]^{2+}$ ($[1]^{2+}$) affording $[\text{Ru}(\text{bpy})_2(\text{pbnH}_2)]^{2+}$ in the presence of $\text{N}(\text{CH}_2\text{CH}_2\text{OH})_3$ (eq 2). Photochemical two-electron reduction of $[\text{Ru}(\text{bpy})_2(\text{pbn})]^{2+}$ proceeds via (i) reductive quenching of photo-excited $[\text{Ru}(\text{bpy})_2(\text{pbn})]^{2+*}$ by $\text{N}(\text{CH}_2\text{CH}_2\text{OH})_3$, (ii) subsequent protonation of free nitrogen of the anion radical pbn ligand of $[\text{Ru}(\text{bpy})_2(\text{pbn}^{\bullet-})]^+$, (iii) inter-molecular π - π adduct formation between two neutral pbnH[•] of the resultant $[\text{Ru}(\text{bpy})_2(\text{pbnH}^{\bullet})]^+$, and (iv) disproportionation of $\{[\text{Ru}(\text{bpy})_2(\text{pbnH}^{\bullet})]^+\}_2$ affording an equimolar mixture of $[\text{Ru}(\text{bpy})_2(\text{pbnHH})]^{2+}$ and $[\text{Ru}(\text{bpy})_2(\text{pbn})]^{2+}$. The finding of the path for

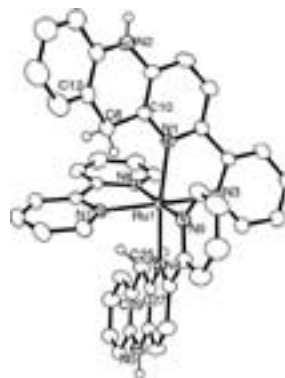


Figure 2. Crystal structure of $[\text{Ru}(\text{bpy})(\text{pbnH}_2)]^{2+}$.

the two-electron reduction driven us to repeat the two-electron reduction of pbn of $[\text{Ru}(\text{bpy})(\text{pbn})_2](\text{PF}_6)_2$ ($[2](\text{PF}_6)_2$) and $[\text{Ru}(\text{pbn})_3](\text{PF}_6)_2$ ($[3](\text{PF}_6)_2$) to achieve the first photochemical four- and six-electron reductions of monomeric metal complexes.

The molecular structure of $[2](\text{PF}_6)_2$ (Figure 2) has a C_2 symmetry. Although many attempts to grow single crystal of $[3](\text{PF}_6)_2$ for X-ray diffraction study were not succeeded, an appearance of 33 proton signals in the aromatic region in the ^1H NMR spectrum implied the formation of a single stereo isomer of $[3]^{2+}$. Low energy level of π^* orbital of pbn of $[1]^{2+}$, $[2]^{2+}$ and, $[3]^{2+}$ reflects their redox potentials; they showed one (-1.07 V vs Ag/AgNO_3), two (-1.01 and -1.14 V), and three (-0.94 , -1.11 , and -1.31 V) pbn localized reversible (pbn/pbn^{•-}) redox couples in the cyclic voltammogram. Irradiation of visible light to $[2](\text{PF}_6)_2$ and $[3](\text{PF}_6)_2$ in $\text{CH}_3\text{CN}/\text{N}(\text{CH}_2\text{CH}_2\text{OH})_3$ (4 : 1, v/v) smoothly produced $[2\cdot\text{H}_4]^{2+}$ and $[3\cdot\text{H}_6]^{2+}$ with time.

References

- 1) K. Kimura and K. Tanaka, *Angew. Chem., Int. Ed.* **47**, 9768–9771 (2008).
- 2) D. Polansky, D. Cabelli, J. Muckerman, T. Fukushima, K. Tanaka and E. Fujita, *Inorg. Chem.* **47**, 3958–3968 (2008).

Visiting Professors



Visiting Professor
ITOH, Shinobu (*from Osaka University*)

Dioxygen Activation Mechanism by Copper Proteins and Models

The structure and reactivity of copper/active-oxygen complexes have attracted much interest during the past decades because of their potential relevance to biological systems and numerous copper-catalyzed oxidation reactions. In our laboratory, we have been studying the reactivity of several types of copper/active-oxygen species such as mononuclear copper(II)-superoxo and copper(II)-hydroperoxo complexes as well as dinuclear copper(II)-peroxo and bis(μ -oxo)dicopper(III) complexes in order to evaluate the catalytic mechanism of copper oxygenases and to develop efficient oxidation catalysts for organic synthesis.



Visiting Professor
TAKAHASHI, Satoshi (*from Tohoku University*)

Dynamics of Protein Folding by Single Molecule and Ensemble Techniques

Protein is a linear macromolecule that has a unique property to fold to a specific three-dimensional structure from fully unfolded conformations. We are interested in the physical principles that connect the unfolded and the folded conformations of proteins. To detect fast kinetic processes involved in protein folding, we use rapid mixing device for the time resolved observation of average protein structures. To observe heterogeneity and dynamic fluctuations, we use single molecule observation systems. Based on the ensemble measurements on several proteins using small angle X-ray scattering and circular dichroism spectroscopy, we proposed “collapse and search” mechanism of protein folding. The recent application of single molecule fluorescence measurements clarified a relatively slow conformational dynamics in the unfolded state. We are hoping to obtain important information required for the protein structure prediction and design through the further examination of protein folding dynamics.



Visiting Associate Professor
HASEGAWA, Miki (*from Aoyama Gakuin University*)

Development of the Polarized Emission System of Lanthanide Complexes in the Nano-Thickness Molecular Films

The nano-thickness molecular films containing lanthanide ions induce the polarized emission. The phenomenon is not generally observed from both a fluorescent organic compound and a lanthanide ion. However, we firstly succeeded to construct functional multilayers by the Langmuir-Blodgett (LB) method. The film containing the Pr(III) layer showed the polarized $\pi\pi^*$ emission of the inserted aromatic molecule, which was slightly affected by the interaction with metals. On the other hand, the Eu(III) layer within the film led to the polarized ff-emissions of metal ion itself. The principle should be clarified from the viewpoint of molecular science. We are in progress to reveal the relation between the structure around metals and the photo-phenomena of the lanthanides' LB film.